

E13-2009-170

O. L. Klimov, A. D. Volkov*

MEASUREMENT OF THE CRYOMODULE COLD MASS
DISPLACEMENT USING THE **WPM**

Submitted to «Приборы и техника эксперимента»

*E-mail: volkov@nusun.jinr.ru

Климов О.Л., Волков А.Д.

E13-2009-170

Измерение смещения холодной массы криомодуля
с помощью WPM

В работе развивается методика косвенного измерения смещения холодной массы криомодуля с использованием проволочного позиционного монитора (WPM). Получены аналитические выражения передаточных функций тестового сигнала для WPM. Определены зависимости величин смещения x , y холодной массы как функции амплитуды сигналов с координатных электродов и параметров монитора. Функции смещения не зависят от амплитуды тестового сигнала и применимы в диапазоне отклонения $r \leq 0,82R$. Результаты представляют интерес для определения смещения холодной массы криомодуля в ускорителях нового поколения, таких как ILC, NICA, FAIR, XFEL.

Работа выполнена в Лаборатории ядерных проблем им. В.П. Джелепова ОИЯИ.

Препринт Объединенного института ядерных исследований. Дубна, 2009

Klimov O.L., Volkov A.D.

E13-2009-170

Measurement of the Cryomodule Cold Mass Displacement
Using the WPM

A method for indirect measurement of the cryomodule cold mass displacement using the wire position monitor (WPM) is developed in the work. An analytical expression for the transfer functions of the test signal is obtained for the WPM. Dependences of the x , y coordinates of the cold mass displacement upon the amplitude of the electrode signals and the parameters of the monitor are determined. The displacement functions are applicable in the deviation range $r \leq 0.82R$ and do not depend upon the test signal amplitude. The results are of interest for the monitoring of the beam position and the cryomodule cold mass displacement in new-generation accelerators like ILC, NICA, FAIR and XFEL.

The investigation has been performed at the Dzhelepov Laboratory of Nuclear Problems, JINR.

Preprint of the Joint Institute for Nuclear Research. Dubna, 2009

INTRODUCTION

The new technology of particle beam acceleration in modern accelerators is based on the use of cryomodules [1]. Cryomodule elements operating in the temperature range 2–8 K are called the cold mass. They are strongly affected by temperature, and their position in space should therefore be continuously monitored. The design features and operation conditions of the cryomodules do not allow direct measurement of their displacement in the course of operation. Wire position monitors (WPMs) [2–6] allowing indirect determination of the displacement have found wide use as position sensors. A change in the position of the cryomodule cold mass in the transverse XY plane is found from the displacement functions describing its value depending on the amplitudes of signals from the coordinate electrodes of the monitor. The longitudinal displacement is compensated by the bellows connection and is not detected. The displacement functions given in [4, 7] have limitations on the value and determination accuracy of this displacement. This induced the authors to perform the calculations and eliminate the disadvantages mentioned. An important condition for determination of the displacement is that the signals should not be distorted by the detection system in the course of measurement. To this end, a circuit for matched connection of the WPM coordinate electrodes into the measurement system was developed. The conclusions drawn in the work are confirmed by the data of measurements represented by A. Bosotti, INFN, Milano, Italy.

POSITION MONITOR

A cylinder-shaped WPM is considered in the paper. It is schematically depicted in Fig. 1. The monitor consists of metallic cylinder with the radius R , four coordinate electrodes A – D performed in form of strips and 500 μm beryllium bronze wire. Strips are located near the inner surface of cylinder. They are arranged orthogonally to the XY plane and are about 10 cm long. Electrodes A and C serve to determine displacement in the Y direction, and electrodes B and D serve to determine displacement in the X direction. The WPM receives a signal from the external generator supplied to the wire which is the origin O of the

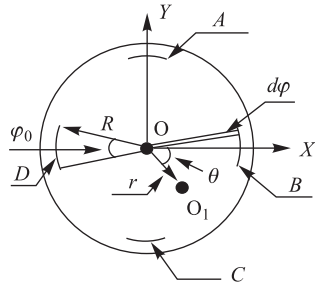


Fig. 1. Structural scheme of the position monitor

special units of the cryomodule which are not affected by the cold mass displacement. One end of the wire is rigidly fixed. The other end carries through a block to the weight 17 kg ensuring the constant tension and allows changing the wire length under the temperature effect.

monitor coordinate system. Outside the monitor the wire is screened by a copper tube, which allows coordination of the signal transfer for other WPMs at the cryomodule. Figure 2 shows the WPM incorporated in the measuring system.

The test signal causes a reversed-polarity current in the inner surface of the tube and the monitor cylinder. Part of this current is divided into the coordinate electrodes. The value of the current in the strip depends upon its size and position with respect to the wire. The monitor cylinder is rigidly fastened to the cold mass of the cryomodule that is subject to displacement. The wire is fastened to

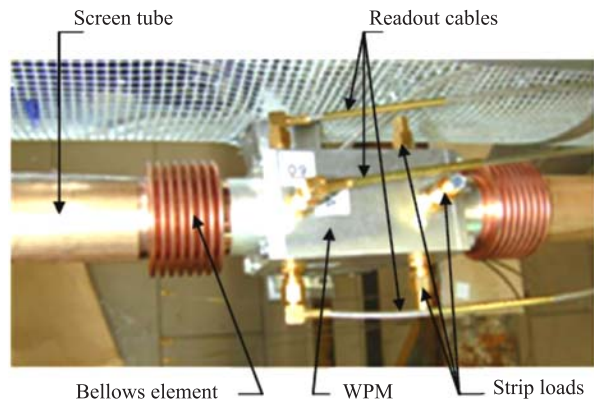


Fig. 2. WPM measuring system

TRANSFER FUNCTIONS OF THE MONITOR

Transfer functions show which part of the test signal is fed to the coordinate electrodes in relation to the amount of displacement and their size. Ultimately, they allow the amount of the cold mass displacement to be calculated. The analytical finding of transfer functions involves calculation of the Poisson integral. The integral describes the current on the inner surface of the monitor

within angular width φ when it is shifted by r at the angle θ with respect to the center of the monitor. The designations used below are shown in Fig. 1. For the problem in question, the current in the strip I_S within its angular width φ_0 is defined by the integral:

$$I_S = \frac{I_0}{2\pi} \int_{-\varphi_0/2}^{\varphi_0/2} \frac{R^2 - r^2}{R^2 + r^2 - 2Rr \cdot \cos(\theta - \varphi)} d\varphi, \quad (1)$$

where I_0 is the amplitude of the test signal. With the replacement $c = r/R$, $b = 2c/(1 + c^2)$, the integral is reduced to the tabulated form:

$$I_S = \frac{I_0}{2\pi} \cdot \frac{1 - c^2}{1 + c^2} \cdot \int_{-\varphi_0/2}^{\varphi_0/2} \frac{d(\varphi - \theta)}{1 - b \cdot \cos(\varphi - \theta)} = \frac{I_0}{2\pi} \cdot 2 \operatorname{arctg} \frac{1 - c}{1 + c} \cdot \operatorname{tg} \frac{\varphi - \theta}{2} \Big|_{-\varphi_0/2}^{\varphi_0/2}. \quad (2)$$

After trigonometric transformations the integral for strip B is

$$I_B \approx \frac{I_0}{2\pi} \cdot 2 \operatorname{arctg} \frac{(1 - c^2) \cdot \varphi_0}{2(1 + c^2 - 2c \cdot \cos \theta)}. \quad (3)$$

Since the monitors in question have the angle φ_0 no larger than 12° , the approximations $2 \sin(\varphi_0/2)$ and $\cos(\varphi_0/2) \approx 1$ were used for calculating (3). The transfer functions for other strips are expressed by the relations:

$$I_D \approx \frac{I_0}{2\pi} \cdot 2 \operatorname{arctg} \frac{(1 - c^2) \cdot \varphi_0}{2(1 + c^2 + 2c \cdot \cos \theta)}, \quad (4)$$

$$I_A \approx \frac{I_0}{2\pi} \cdot 2 \operatorname{arctg} \frac{(1 - c^2) \cdot \varphi_0}{2(1 + c^2 - 2c \cdot \sin \theta)}, \quad (5)$$

$$I_C \approx \frac{I_0}{2\pi} \cdot 2 \operatorname{arctg} \frac{(1 - c^2) \cdot \varphi_0}{2(1 + c^2 + 2c \cdot \sin \theta)}. \quad (6)$$

DISPLACEMENT FUNCTIONS

Displacement functions allow the amount of displacement to be found from the measured amplitudes of the signals from the coordinate electrodes. To this end, the system of Eqs. (3)–(6) should be solved for the displacements in the X and Y directions. To avoid the influence of the test signal amplitude, the dimensionless quantities D_x and D_y are introduced in the calculation of the displacement functions:

$$D_x = \frac{I_B - I_D}{I_B + I_D}, \quad D_y = \frac{I_A - I_C}{I_A + I_C}. \quad (7)$$

In practice, one usually measures strip voltage U_S equal to the product of the current I_S and the readout amplifier load resistance Z_L . Considering (3) and (4),

$$D_x = \frac{\operatorname{arctg} \frac{(1-c^2) \cdot \varphi_0}{2(1+c^2-2c \cdot \cos \theta)} - \operatorname{arctg} \frac{(1-c^2) \cdot \varphi_0}{2(1+c^2+2c \cdot \cos \theta)}}{\operatorname{arctg} \frac{(1-c^2) \cdot \varphi_0}{2(1+c^2-2c \cdot \cos \theta)} + \operatorname{arctg} \frac{(1-c^2) \cdot \varphi_0}{2(1+c^2+2c \cdot \cos \theta)}}. \quad (8)$$

At the given angle $\varphi_0 \approx 0.1929$ (12°) and in the interval $c \leq 0.82$ the arguments of the arctg functions in (8) are smaller than unity. In this interval the arctg functions can be expanded in the Taylor series. Using the first expansion term $\operatorname{arctg}(z) \approx z$ alone, we get

$$D_x \approx \frac{2c \cdot \cos \theta}{1+c^2} \cdot \left\{ 1 - \frac{(1-c^2)^2 \cdot \varphi_0^2}{2[(1+c^2)^2 - 4c^2 \cdot \cos^2 \theta]} \right\}. \quad (9)$$

Similar calculations of D_y yield

$$D_y \approx \frac{2c \cdot \cos \theta}{1+c^2} \cdot \left\{ 1 - \frac{(1-c^2)^2 \cdot \varphi_0^2}{2[(1+c^2)^2 - 4c^2 \cdot \sin^2 \theta]} \right\}. \quad (10)$$

Despite the simplicity of resulting expressions (9) and (10), their calculation involves cumbersome trigonometric transformations and has been brought to the ultimate result for the first time. The contribution from the term with φ_0^2 is the largest in the case of displacement in the X or Y direction and runs to $\varphi_0^2/2$. Since only narrow strips are used in the monitors, this value is not larger than 2%. Therefore, in practice, one can use the approximations:

$$D_x \approx \frac{2x}{1+x^2+y^2}, \quad (11)$$

$$D_y \approx \frac{2y}{1+x^2+y^2}, \quad (12)$$

where the relative displacement along the axes is defined by the relations:

$$x = c \cdot \cos \theta, \quad y = c \cdot \sin \theta.$$

The cold mass displacement functions along X and Y directions can be found in the analytical form by solving the system of Eqs.(11) and (12):

$$x = D_x \cdot \frac{\left(1 - \sqrt{1 - D_x^2 - D_y^2}\right)}{D_x^2 + D_y^2}, \quad y = D_y \cdot \frac{\left(1 - \sqrt{1 - D_x^2 - D_y^2}\right)}{D_x^2 + D_y^2}. \quad (13)$$

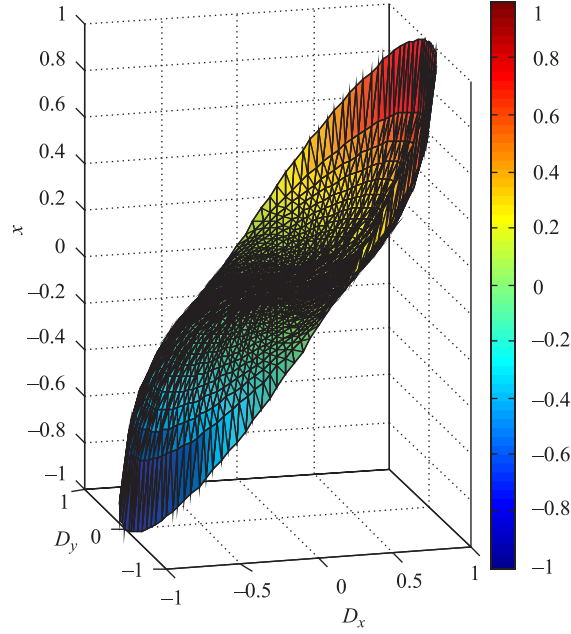


Fig. 3. Displacement x as a function of D_x and D_y

The displacements are no larger than unity at all permissible values of D_x and D_y , which indicates that the obtained relations are applicable in the entire displacement interval $r < R$. It should be mentioned that D_x , D_y are interdependent: $D_x^2 + D_y^2 \leq 1$. Figure 3 shows the behavior of the displacement function x with variation in D_x and D_y . The function in the displacement range $r \leq 0.2R$ is linear and asymptotically approaches unity as $r \rightarrow R$. The behavior of the displacement function y has a similar form. Only numerical methods allow more accurate calculation of the displacements using expressions (9) and (10). In this case there arises a system of equations of the sixth degree that has no analytical solution. Numerical solution of the system of Eqs.(9) and (10) using the MATLAB-2007b code takes several seconds and can be performed in the on-line mode.

CONNECTION OF THE MONITOR INTO THE MEASURING SYSTEM

Requirements on the connection of the WPM strips into measurement circuit are formulated in [7]. A source of signals for the WPM is the external

generator (Gen) from which a continuous sinusoidal signal of constant frequency 100–150 MHz and amplitude 1–8 V is applied to the wire. In the measuring system the strip shields part of the inner surface of the cylinder. To prevent reflections of the signal induced on the strip and to retain the amplitude, strip should be matched. To this end, the ends of the strip should be loaded with the line wave resistance Z_{TL} . The other ends of the load resistor are connected to the grounded cylinder. The value Z_{TL} depends upon the monitor radius R , the wire radius d , and the displacement $r = OO_1$. The majority of monitors have Z_{TL} ranging between 150–250 Ω . It should be stressed that the inner diameters of the screen tube and the WPM cylinder should coincide to ensure constant Z_{TL} .

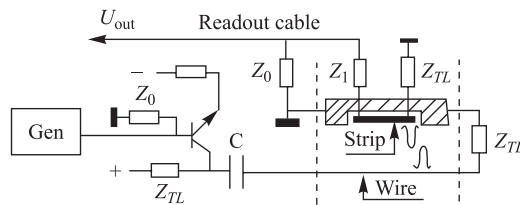


Fig. 4. Circuit diagram of the matched strip connection

When the signal to be detected is transferred through the cable with the wave resistance $Z_0 = 50 \Omega$, there must be a matching load at the input end. It is taken into account in the matching of the strip. The connection of the strip into the measurement circuit recommended by the authors is shown in Fig. 4. The end of the strip from which the signal is read out is matched using Z_0 and the compensating resistor Z_1 in the relation $Z_1 = Z_{TL} - Z_0$. A resistor Z_{TL} is connected to the opposite end of the strip. Since temperature variations during the operation of the cryomodule affect the value Z_{TL} , it is reasonable to connect the load Z_{TL} to the test signal input as well. It will suppress repeated reflections of the signals at not ideal matching of strips. In the circuit, the test signal arrives at the wire through the buffer transistor follower and the separating capacitor C . The collector output of the follower allows its load to be used for matching the transmission line and the mutual influence of the excitation and readout circuits to be avoided.

EXPERIMENTAL VERIFICATION OF THE DISPLACEMENT FUNCTIONS

Correctness of the displacement functions (13) obtained for the WPM was checked on the test bench. The monitor was attached to the coordinate table which allowed its movement with respect to the wire in the XY plane accurate to 1 μm . The tested WPM has the radius $R = 14 \text{ mm}$ and strips wide 2.7 mm ($\varphi_0 \cong 0.1929$). Signals from the coordinate electrodes were amplified and then digitized using 14-bit converters. The amplification gain was 10. The shift of the converters' zero was taken into account in the calculation of D_x and D_y .

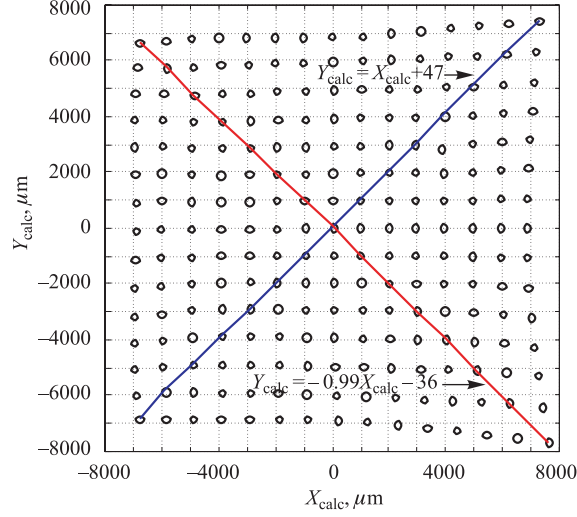


Fig. 5. Map of calculated WPM displacements

Amplitudes of signals were measured with a step of 1 mm along each coordinate axis in the interval ± 7 mm. The X coordinate always changed in one direction from -7 to $+7$ mm. At each value of X the value of Y was varied from the minimum to the maximum. Then, the value of X was increased and measurement of amplitudes continued at the back displacement in the Y direction. This procedure decreased the clearance of the micrometric screws setting the displacement.

The values D_x , D_y were measured at the every coordinate point. Then, displacements were calculated by formulas (13) and compared with the settled X_M , Y_M coordinates. Measurement of D_x and D_y also allows the monitor making quality to be evaluated. In Fig. 5, the values X_{calc} and Y_{calc} are shown by circles. The monitor coordinates are at the nodes of the coordinate grid. The diagonal points of the measurement array are described by the linear relations with the maximum deviation from the lines in $64 \mu\text{m}$:

$$Y_{\text{calc}} = X_{\text{calc}} + 0.047, \quad Y_{\text{calc}} = -0.99X_{\text{calc}} - 0.036.$$

The transformation coefficient of the second curve is -0.99 , which indicates that the slope of the Y axis is 0.3° . The straight lines are seen to be shifted in the Y direction by $+47$ and $-36 \mu\text{m}$, respectively. The Table presents examples of measurements indicating the disagreement between the coordinates systems of the monitor and the displacement table.

The first two lines show the shift of the zero on the repeated passage through it, which was as large as $30 \mu\text{m}$. Lines 3–4 show the positive-direction shift of

N	D_x	D_y	X_M , mm	Y_M , mm	X_{calc} , mm	Y_{calc} , mm
1	-0.00042	0.004246	0	0	-0.003	0.0297
2	-0.00163	0.004064	0	0	-0.011	0.0284
3	0.669484	0.68504	7	7	7.281	7.450
4	0.682905	-0.68505	7	-7	7.626	-7.650
5	-0.66109	-0.66057	-7	-7	-6.828	-6.821
6	-0.6656	0.649562	-7	7	-6.814	6.650

the Y axis of the monitor with respect to the coordinate table. It is confirmed by the values of D_x and D_y . At the identical shift of the X axis and symmetrical deviation in the Y direction the values of D_y should differ only in sign and the values of D_x should coincide. The difference between the values of D_y in lines 5–6 may indicate rotation of the Y axis of the monitor, which agrees with the diagonal data fits. As it is evident from Fig. 5, the deviations $\Delta x = X_M - X_{\text{calc}}$ and $\Delta y = Y_M - Y_{\text{calc}}$ are nonsymmetrical and increase with increasing displacement. The possible reasons of the differences Δx , Δy are imperfection of the measuring system and nonideality of the WPM. The values of D_x and D_y for the points arranged symmetrically about the coordinate axes should differ only in sign. The displacements X_{calc} , Y_{calc} obtained from solution of the system of Eqs. (9) and (10) show a smaller deviation from X_M , Y_M than the same values calculated with (13). When the displacement is 7 mm, the deviation runs to the largest value of 45 μm .

CONCLUSIONS

Important issues of using wire position monitors as sensors for displacement of cold mass of cryomodules are considered in the paper. An appreciable contribution to the development of this method is the obtaining of the transfer functions of the test signal for the WPM. This made it possible to obtain for the first time the analytical dependence of the WPM displacement functions allowing one to calculate its value with micron accuracy in a wide range $r \leq 0.82R$. The analysis of the experimental data shows that micron accuracy in determination of the displacement is obtained by using 14-bit amplitude converters and calibrating monitor characteristics, such as orthogonality of coordinate electrodes, identity of their width, and distance to the center of the monitor. The verification results show good agreement with the theoretical description of the wire monitor operation. The deviation of the calculated displacement values is no larger than 3.6% when (13) is used and 2.8% when the system of Eqs. (9) and (10) is numerically solved, except for the points indicated in the table. A scheme for matched con-

nection of the WPM into the measuring system is worked out, which increases the amplitude of the detected signals. The results are of interest for the monitoring of the beam position and the cryomodule cold mass displacement in new-generation accelerators like ILC, NICA, FAIR and XFEL.

Acknowledgements. The authors are grateful to A. Bosotti for representing the data of WPM test.

REFERENCES

1. *Pagani C.* The Cold Technology and TESLA TDR // 2005 Intern. Workshop — Summer School.
www.srf.mil.infn.it/schools-tutorials
2. *Assmann R., Montag C., Salsberg C.* Beam Line Stability Measurements with a Stretched Wire System in the FFTB. SLAC-PUB-7303, 1996.
3. *Giove D. et al.* A Wire Position Monitor (WPM) System to Control the Cold Mass Movements inside the TTF Cryomodule.
www.epics.org/cryomodule/7P06.pdf, 1997.
4. *Bosotti A., Pagani C., Varisco G.* On Line Monitoring of the TTF Cryostat Cold Mass with Wire Position Monitors.
www.epics.org/cryomodule/INFN-TC-00-02.pdf/, INFN/TC-00/02, 2000.
5. *Bosotti A. et al.* Analysis of the Cold Mass Displacement at the TTF // Proc. of the EPAC'04, Lucerne, July 2004. P. 1681.
6. *Bedeschi F. et al.* A New Wire Position Monitor Readout System for ILC Cryomodule // IEEE Trans. Nucl. Sci. 2007. N24-412. P. 1684-1686.
7. *Shafer R.E.* Characteristics of Directional Coupler Beam Position Monitor // IEEE Trans. Nucl. Sci. 1985. NS-32, No. 5. P. 1933-1937.

Received on November 5, 2009.

Редактор *В. В. Булатова*

Подписано в печать 11.12.2009.

Формат 60 × 90/16. Бумага офсетная. Печать офсетная.

Усл. печ. л. 0,75. Уч.-изд. л. 1,01. Тираж 305 экз. Заказ № 56823.

Издательский отдел Объединенного института ядерных исследований
141980, г. Дубна, Московская обл., ул. Жолио-Кюри, 6.

E-mail: publish@jinr.ru

www.jinr.ru/publish/